Sol–gel derived nano-structured zinc oxide film for sexually transmitted disease sensor

Anees A. Ansari,* Renu Singh, G. Sumana and B. D. Malhotra*

Received 6th October 2008, Accepted 19th February 2009
First published as an Advance Article on the web 6th March 2009
DOI: 10.1039/b817562d

A 20-mer thiolated oligonucleotide probe (th-ssDNA) specific to *Neisseria gonorrhoeae* immobilized onto a sol–gel derived nano-structured zinc oxide (ZnO) film dip-coated onto an indium-tin-oxide (ITO) glass substrate has been used for the fabrication of a DNA biosensor for sexually transmitted disease (gonorrhoea) detection using hybridization technique. The results of characterization studies carried out on this th-ssDNA–ZnO/ITO bioelectrode using X-ray diffraction, UV-Visible, Fourier-transform infrared, scanning electron microscopy and electrochemical techniques reveal the linearity as 0.000524 fmol–0.524 nmol, with a detection limit of 0.000704 fmol within 60 s.

Introduction

Gonorrhoea is currently the second most common bacterial sexually transmitted disease (STD). It is estimated that there are about 25 million cases of gonorrhoea worldwide.[1] To prevent spread of this disease, increased attention is being focused on the early diagnosis and treatment of symptomatic or asymptomatic infected individuals. Traditional laboratory diagnosis of this infection is carried out by culture, microscopy and PCR techniques. However, these diagnostic methods are expensive, time-consuming (14–72 h) and are not reliable.[2,3] Therefore, efforts are being made towards the development of a rapid, sensitive and specific STD-sensing device.

Electrochemical DNA biosensors based on nucleic acid hybridization have received considerable attention due to their potential application for the diagnosis of various diseases.[4–12] Many approaches have been followed for the fabrication of electrochemical nucleic acid biosensors. The nano-structured metal oxides offer unique opportunities for electrochemical transduction of DNA-sensing events.[9,12,13] Feng *et al.* have fabricated nano-porous cerium oxide (CeO_2)/chitosan composite film for detection of cancerous DNA sequence by an electrochemical method.[13] In another approach, a nucleic acid sensor has been fabricated using a single-stranded DNA-immobilized MWCNT–nano ZrO_2–chitosan-modified glassy carbon electrode.[12,13] Liu *et al.* have recently reported application of a nano-structured ZnO/chitosan composite film-modified electrode for detection of DNA hybridization.[14]

Many methods such as adsorption, covalent coupling and electrochemical entrapment have been reported for the immobilization of DNA onto given solid substrates under desired conditions. The sol–gel method is considered particularly attractive for the development of a desired biosensor. This is because sol–gel materials can be prepared under ambient conditions and exhibit tunable porosity, high surface area, biocompatibility, excellent thermal stability, chemical inertness and negligible swelling in aqueous and non-aqueous solutions.[15–17] Besides this, a sol–gel derived nano-porous film can retain its bioactivity in a given micro-environment and can be used for direct electron transfer between DNA active sites and the electrode. Many sol–gel metal oxides such as CeO_2,[16,17] tin oxide (SnO_2),[18] titanium oxide (TiO_2),[15] zirconium oxide (ZrO_2)[12] and zinc oxide (ZnO)[19,20] have been utilized for the construction of DNA and enzyme-based biosensors.

We report results of studies on the application of a sol–gel derived nano-structured ZnO film deposited onto indium-tin-oxide (ITO) glass for the fabrication of a DNA biosensor for detection of *Neisseria gonorrhoeae*.

Experimental

Zinc acetate dihydrate, Triton X-100, Tris buffer, ethylenediaminetetraacetic acid (EDTA), potassium monohydrogen phosphate, potassium dihydrogen phosphate, methylene blue, and *N. gonorrhoeae* oligonucleotide probes were procured from Sigma-Aldrich (USA). NH_4OH, HNO_3, solvents and reagents were purchased from Merck India Ltd, Mumbai, India. All the solutions and glass wares were autoclaved prior to being used and desired reagents (molecular biology grade) were prepared in de-ionized water (Milli Q 10 TS). ITO-coated glass substrates were obtained from Balzers, UK. Probes used for the studies include: 5′-thiol end-labeled probe (20-mer) specifically targeting the *Opa* gene (a multi copy gene) of *N. gonorrhoeae*, a complementary target sequence. The sequences of DNA probes used for electrochemical DNA hybridization detection are as follows:

- **Probe**: thiol-5′-CCGGTGCTTCATCACCTTAG-3′;
- **Complementary target**: 5′- CTAAGGTGATGAAG-CACCGG -3';
- **Non-complementary target**: 5′- GTATGGTGAT-CAAGCTCCCG -3′.

Firstly, 1 g of zinc acetate dihydrate [$Zn(CH_3COO)_2 \cdot 2H_2O$] is dissolved in 10 ml distilled de-ionized water. Then 1 ml (1 M) of ammonium hydroxide solution (NH_4OH) is added drop wise to this solution with constant stirring for 4 h at 25 °C to maintain pH

Department of Science & Technology Centre on Biomolecular Electronics, National Physical Laboratory, Dr. K S Krishnan Marg, New Delhi 110012, India. E-mail: bansi.malhotra@gmail.com; aneesaansari@gmail.com; Fax: +91-11-45609310; Tel: +91-11-4560915

8–9. A white milky precipitate of $Zn(OH)_2$ thus obtained is washed with de-ionized water until neutral pH is achieved.[17] Subsequently, dilute HNO_3 (1 M) is added to the precipitate at 25 °C to obtain a solution of pH 1. A transparent sol thus obtained is used to fabricate the thin film on an ITO glass plate *via* dip coating. To achieve a uniform coating on the ITO electrode, 2 wt% Triton X-100 surfactant is added to the resulting solution. These films are then allowed to dry at 400 °C for about 20 minutes.

The ZnO/ITO surface is washed and subject to 5 minutes incubation for physisorption of the 20-mer thiolated oligonucleotide probe (th-ssDNA, 1 ng/ml) specific to *N. gonorrhoeae* in a humid chamber at 25 °C. This ZnO/ITO film is subsequently washed with buffer and dried in a nitrogen environment. The prepared th-ssDNA–ZnO/ITO film bioelectrode is stored at 4 °C when not in use. The sol–gel derived nano-structured ZnO/ITO and th-ssDNA–ZnO/ITO electrodes have been characterized by UV-Visible (Phoenix), SEM (SEM, LEO 440) and Fourier-transform infrared (FTIR) spectrophotometer (Perkin-Elmer, Model 2000) in the wavelength range 400–4000 cm^{-1}. Electrochemical data have been obtained using an Autolab Potentiostat/Galvanostat (Eco Chemie, Netherlands) using a three-electrode system with ITO as the working electrode, platinum wire as the auxiliary electrode, and Ag/AgCl electrode as the reference electrode in phosphate buffer saline (PBS) solution containing 5 mM $[Fe(CN)_6]^{3-/4-}$. The th-ssDNA–ZnO/ITO electrode has been optimized for hybridization time and is subject to incubation in 5 μl of DNA solution in the concentration range (0.000524 fmol–0.524 nmol) of complementary target solution for 60 s at 25 °C. The proposed mechanism of the probe DNA immobilization onto ZnO/ITO and hybridization with target DNA for the detection of *N. gonorrhoeae* is shown in Scheme 1. It has been found that one-minute incubation in target sample solution is sufficient for the hybridization process (data not shown). CV and DPV measurements of the th-ssDNA–ZnO/ITO electrode have been carried out using 20 μM methylene blue (MB), in 0.05 M PBS, pH 7.0, containing 0.9% NaCl.

Results and discussion

Characterization of the sol–gel derived nano-structured ZnO film

The XRD diffraction pattern (Fig. 1A) shows a crystallographic phase present in the sol–gel derived ZnO film deposited on the glass substrate. A high degree of preferential orientation is evident, giving rise to spectra resembling a single crystal diffraction pattern. The prepared film shows (100), (002), (101), (102), (110), (103) and (112) diffraction planes corresponding to the hexagonal wurtzite ZnO structure and well-matched with the standard (JCPDS #751526) data.[19,21] The ZnO film coated onto the glass substrate shows three strong diffraction peaks at (100), (002) and (101), indicating distribution of ZnO grains in the film along different directions. This may be attributed to optimized deposition and annealing of the ZnO film. The diffraction peaks of ZnO are broad suggesting a smaller crystalline size of ZnO. The thickness of the ZnO film is 325 nm. The average crystallite size of the ZnO film calculated by Scherrer's equation is 3.2–5 nm (Fig. 1A). The values of the lattice constants of the ZnO film calculated from the peak position are found to be $a = 3.495$ Å and $c = 5.25$ Å, which are slightly higher than those of the bulk ZnO ($a = 3.249$ Å and $c = 5.202$ Å). The higher value of the lattice constant may be attributed to the fact that the unit cell is slightly elongated along the growth direction. In addition, increase in the lattice constant reveals a lattice expansion effect resulting from increased oxygen vacancies and Zn^{2+} ions with decreased particle size.

Fig. 1B shows UV-Visible spectra obtained for the sol–gel derived nano-structured ZnO and th-ssDNA–ZnO film. It can be seen that the observed absorption maximum (371 nm) of the nano-structured ZnO film (curve a) is blue shifted to 345 nm with increased intensity after DNA immobilization, indicating immobilization *via* electrostatic interactions between negatively charged th-ssDNA and positively charged ZnO (curve b).[22]

The SEM image (Fig. 1C) of ZnO/ITO shows a uniformly distributed porous three-dimensional structure that is conducive for the immobilization of oligonucleotides [Fig. 1C(i)]. Upon immobilization of DNA, the porous structure of the ZnO/ITO film becomes globular containing light/bright streaks. The globular morphology is attributed to the immobilization of DNA biomolecules onto the free volume of ZnO/ITO whereas bright/light streaks are assigned to the charged DNA molecules [Fig. 1C(ii)]. The immobilization of DNA onto ZnO/ITO occurs due to high isoelectric point (IEP) of ZnO (9.5) that is suitable for adsorption of low IEP DNA (IEP 4.2). At the physiological pH 7.5, the positively charged ZnO matrix not only provides a biocompatible environment for immobilizing negatively charged DNA molecules, but also promotes electron transfer between DNA and the electrode[19]

Electrochemical studies of the ZnO/ITO electrode, th-ssDNA–ZnO/ITO bioelectrode and th-dsDNA-ZnO/ITO bioelectrode

Fig. 2A shows results of cyclic voltammetry (CV) measurements carried out on the bare ITO electrode, ZnO/ITO electrode, th-ssDNA–ZnO/ITO bioelectrode and th-dsDNA-ZnO/ITO bioelectrode in PBS (50 mM, pH 7.0, 0.9% NaCl) containing 5 mM

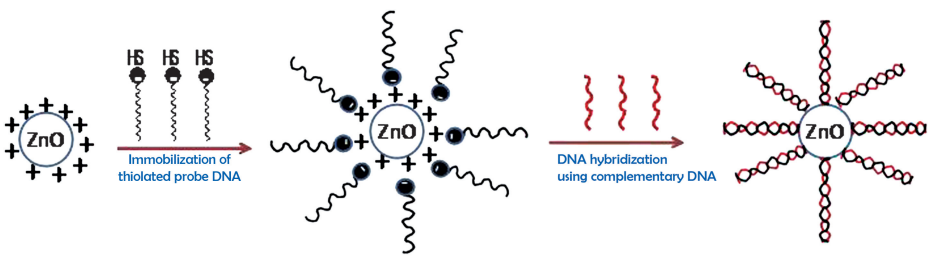

Scheme 1 Sol–gel derived ZnO-based STD sensor for the detection of *N. gonorrhoeae*.

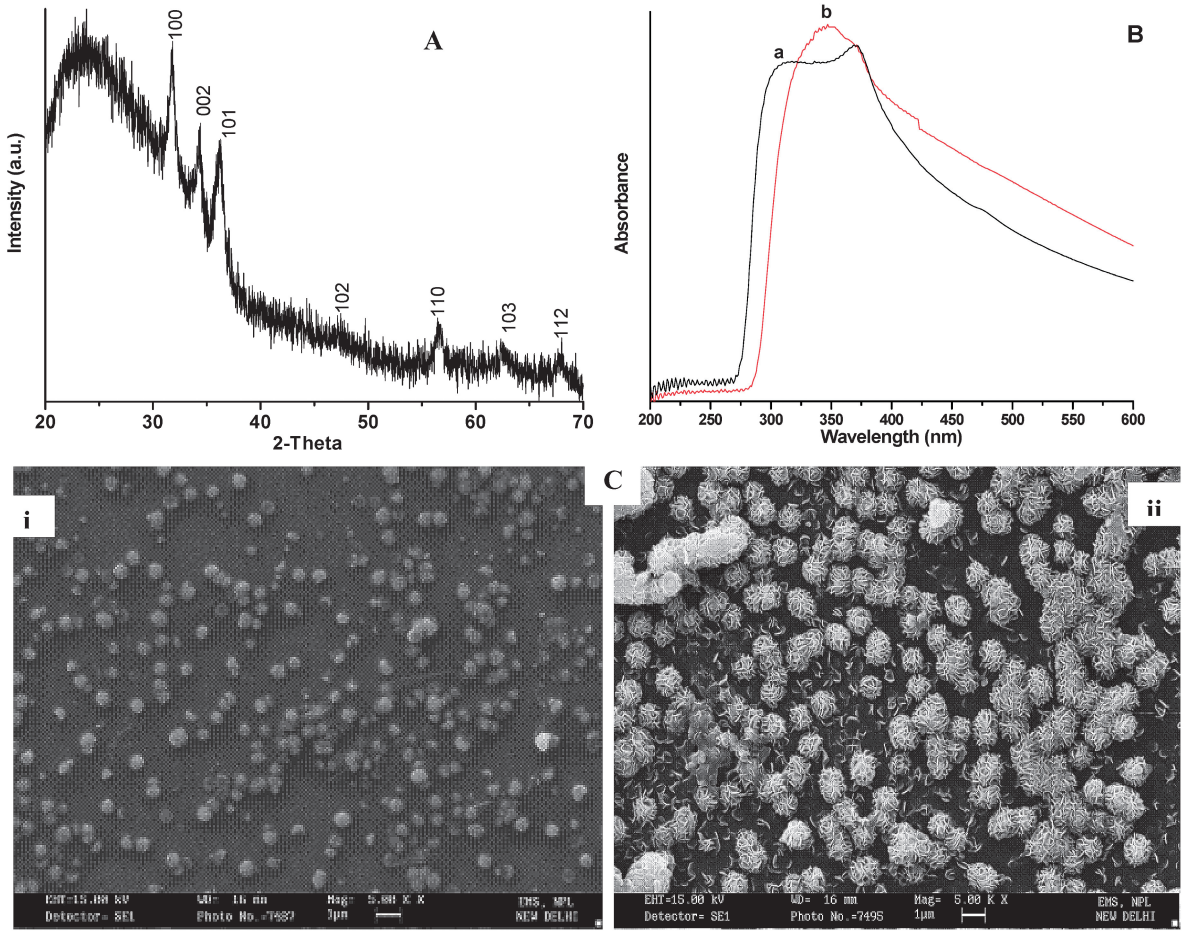

Fig. 1 (A) X-Ray diffraction pattern of sol–gel derived nano-structured ZnO film. (B) UV-Vis spectra of (a) sol–gel derived nano-structured ZnO/ITO electrode and (b) th-ssDNA–ZnO/ITO bioelectrode. (C) SEM micrograph of (i) sol–gel derived nano-structured ZnO/ITO electrode and (ii) th-ssDNA/ZnO/ITO bioelectrode.

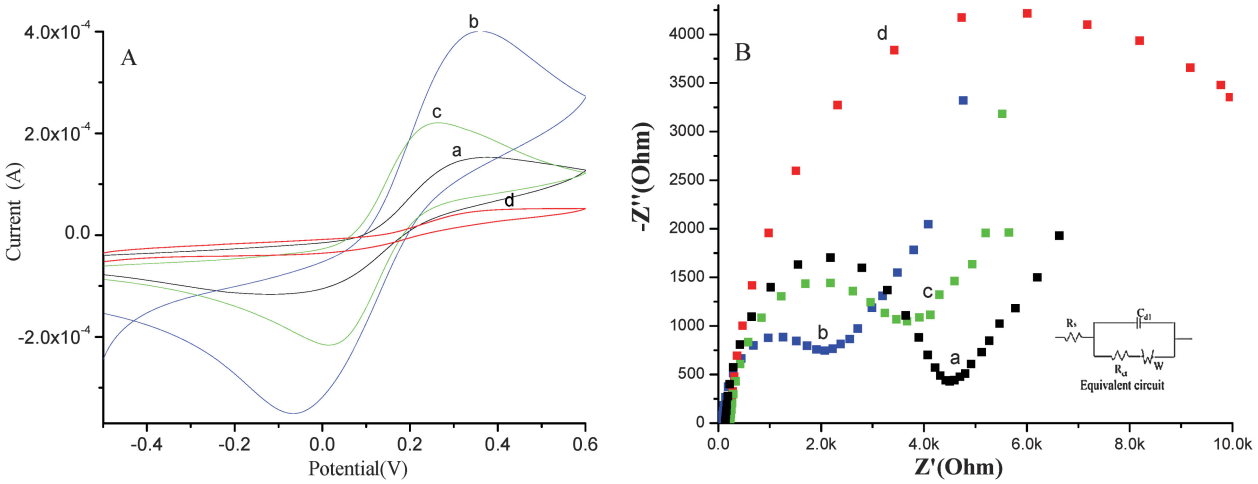

Fig. 2 (A) Cyclic voltammograms of (a) bare ITO electrode, (b) sol–gel derived nano-structured ZnO/ITO electrode, (c) th-ssDNA–ZnO/ITO bio-electrode, and (d) th-dsDNA-ZnO/ITO bioelectrode in PBS (50 mM, pH 7.0, 0.9% NaCl) containing 5 mM $[Fe(CN)_6]^{3-/4-}$ at a scan rate of 50 mV/s. (B) Electrochemical impedance of (a) bare ITO electrode, (b) sol–gel derived nano-structured ZnO/ITO electrode, (c) th-ssDNA–ZnO/ITO bioelectrode, and (d) th-dsDNA-ZnO/ITO bioelectrode in PBS (50 mM, pH 7.0, 0.9% NaCl) containing 5 mM $[Fe(CN)_6]^{3-/4-}$ at a scan rate of 50 mV/s.

$[Fe(CN)_6]^{3-/4-}$ at a scan rate of 50 mV/s, respectively. The CV of the bare ITO electrode (curve a) shows a well-defined cathodic peak at −0.0544 V and an anodic peak at 0.356 V in the potential range of 0.6 to –0.50 V. However, significant enhancement (curve b) in the peak potential [cathodic peak potential (E_{pc}) to −0.064 V and anodic peak potential (E_{pa}) to 0.353 V] is observed after the sol–gel ZnO film is deposited. The considerable enhancement in peak current may be attributed to increased electrical conductivity due to ZnO nanoparticles. However, after immobilization of th-ssDNA onto the ZnO electrode, the peak current decreases. The cathodic and anodic peak potentials are observed at −0.0135 and 0.0257 V, respectively, implying the immobilization of th-ssDNA onto the ZnO electrode. This result can be attributed to electrostatic interactions between polyanionic DNA immobilized onto the sol–gel derived nano-structured ZnO/ITO and the anionic redox couple ions.[12,28] It appears that insulating ssDNA layer self-assembled on the modified electrode surface blocks conducting sites of the ZnO/ITO electrode. After hybridization of the bioelectrode with target DNA, a decrease in the peak current is observed.

Fig. 2B shows results of electrochemical impedance spectroscopy (EIS) measurements carried out as a function of frequency on bare ITO, ZnO/ITO electrode, th-ssDNA–ZnO/ITO and th-dsDNA-ZnO/ITO bioelectrode in the presence of PBS (50 mM, pH 7.0, 0.9% NaCl) containing 5 mM $[Fe(CN)_6]^{3-/4}$. The charge transfer resistance (R_{CT})[6–9] of the ZnO/ITO electrode is found to decrease to 2.21 kΩ as compared to that of the bare ITO electrode (R_{CT} 4.28 kΩ) and lower value of R_{CT} of the ZnO/ITO electrode reveals that ZnO nanoparticles provide an increased electroactive surface for ZnO nanoparticles and enhanced electron transfer. However, when th-ssDNA is immobilized onto ZnO/ITO electrode, R_{CT} of the ZnO/ITO electrode increases to 4.99 kΩ due to presence of electro-negative phosphate skeletons that perhaps prevent $[Fe(CN)_6]^{3-/4-}$ ions from reaching the electrode surface for electron transfer during redox reaction. This reveals that th-ssDNA has been immobilized on the sol–gel derived nano-structured ZnO/ITO electrode. Further increase in R_{CT} of the th-dsDNA-ZnO/ITO bioelectrode may be due to the negatively charged surface of the th-dsDNA-ZnO/ITO bioelectrode that prevents $[Fe(CN)_6]^{3-/4-}$ in solution from clustering on the electrode surface for electron exchange.

The impedance data have been fitted using commercially available software Z_{view}. A modified Randle's equivalent circuit has been used for measurement over the entire measurement frequency range. The circuit, which is often used to model interfacial phenomena, includes (i) ohmic resistance of the electrolyte solution, R_s; (ii) Warburg impedance, Z_w, resulting from the diffusion of ions from the bulk electrolyte to the electrode interface; (iii) the interfacial double layer capacitance (C_{dl}) between an electrode and solution, relating to the surface condition of the electrode, since the surface of the three-dimensional nano-structured ZnO/ITO film is very rough, it has a larger real surface area – we have, therefore, used a constant phase element (CPE) instead of classical capacitance to fit the impedance data, since the electrolyte side of the interface dominates impedance of the interface; and (iv) the electron transfer resistance, R_{CT}, which exists if a redox probe is present in the electrolyte solution.[6,7] The parallel elements (CPE and $Z_w + R_{CT}$) of the equivalent circuit have been introduced since the total current through the working interface is sum of the respective contributions from the Faradaic process and the double layer charging. Ideally, Z_w and R_s represent bulk properties of the electrolyte solution and diffusion of the redox probe in solution.[23,24] A negligible change in R_s is observed during the modification process. As shown in Fig. 2B, it can be seen that ohmic resistance of the solution is not affected by modification of the electrode. Moreover, it can be seen (Fig. 2B) that observed changes in R_{CT} are much larger than those of other impedance components (Table 1).

Table 1 Electrochemical impedance characteristics of the modified ZnO/ITO bioelectrode

S.N.	Electrode	R_s (Ω)	R_{CT} (kΩ)	C_{dl} (μF)	Z_w (μΩ)
1	Bare ITO	1.32	4.28	4.62	8.56
2	Sol–gel ZnO/ITO	6.92	2.21	5.90	8.09
3	th-ssDNA–ZnO/ITO	7.16	4.99	4.60	14.83
4	th-dsDNA-ZnO/ITO	2.26	1.00	5.46	10.22

Amperometric response characteristics of th-ssDNA–ZnO/ITO and th-dsDNA-ZnO/ITO bioelectrodes

Fig. 3A shows the results of differential pulse voltammetry (DPV) measurements carried out on the ITO electrode, th-ssDNA–ZnO/ITO, th-dsDNA-ZnO/ITO and th-ssDNA–ZnO/ITO treated with non-complementary DNA in PBS (50 mM, pH 7.0, 0.9% NaCl) in the presence of methylene blue (MB). MB as an electroactive redox indicator is used for the electrochemical sensing of DNA hybridization at the electrode surface[4,5,12,13] and is known to associate with unpaired nitrogenous bases of ssDNA as compared to dsDNA. Curve a in Fig. 3A is the DPV curve of bared ITO, that has a well-defined peak at around −0.25 V. Curve b is the DPV of the th-ssDNA–ZnO/ITO electrode, indicating strong affinity of MB for free guanine bases and that no duplex/hybrid is formed at the th-ssDNA–ZnO/ITO electrode.[4,5,25] This may be attributed to the positively charged ZnO molecules that may repel positively charged MB molecules facilitating MB molecules to get associated with both partially or unpaired nitrogenous bases of the DNA probe stationed at the th-ssDNA–ZnO/ITO surface. The observed peak seen at −0.25 V may be assigned to the reduction of unpaired nitrogenous bases or to the ZnO matrix. A significant decrease in MB signal is observed when hybridizing with the complementary target sequence (curve c), since interaction of MB and guanine residues of the probe is prevented by duplex formation on the electrode surface.[4,5,25] The observed insignificant change in MB signal on its treatment with the non-complementary target sequence (curve d) indicates non-hybridization.

Fig. 3B describes the results of response studies of th-ssDNA–ZnO/ITO bioelectrode after hybridization with different concentrations of target DNA of *N. gonorrhoeae* ranging from 0.000524 fmol to 0.524 nmol. The absence of the MB peak after hybridization with the complementary synthetic oligomer is attributed to steric inhibition of MB packing between double helix of the hybrid.[4,5,25–27] The DPV peak current of th-ssDNA–ZnO/ITO increases with the decrease in the concentration of target DNA, indicating an enhanced number of double-stranded

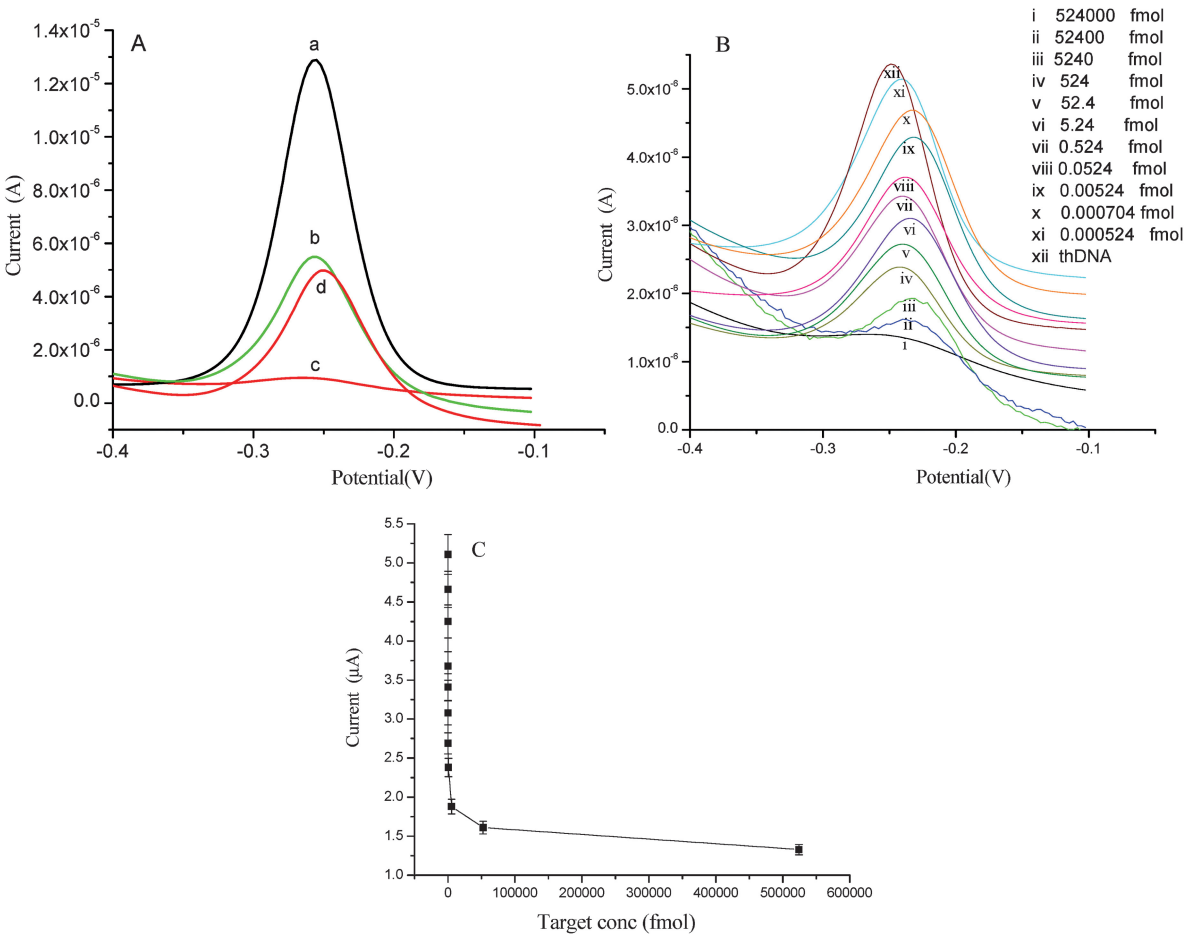

Fig. 3 (A) Differential pulse voltammograms of (a) bare ITO electrode, (b) th-ssDNA–ZnO/ITO bioelectrode, (c) th-dsDNA-ZnO/ITO bioelectrode, and (d) th-ssDNA–ZnO/ITO bioelectrode treated with non-complementary target DNA at a pulse height of 50 mV and pulse width of 70 ms, in 0.05 M phosphate buffer of pH 7.0 containing 0.9% NaCl and methylene blue (MB, 20 μM). (B) Response of the th-ssDNA–ZnO/ITO bioelectrode after hybridization with complementary target probe concentration 0.000524 fmol–0.524 nmol at a pulse height of 50 mV and pulse width of 70 ms, in 0.05 M phosphate buffer of pH 7.0 containing 0.9% NaCl and methylene blue (MB, 20 μM). (C) The MB peak height as a function of target DNA concentration.

DNA molecules at the surface (Fig. 3B). The average current of the DNA bioelectrode is linear with logarithmic value of the complementary sequence concentration range of 0.000524 fmol–0.524 nmol. The detection limit of the th-ssDNA–ZnO/ITO bioelectrode is 0.000704 fmol with a hybridization time of 60 s.

The decrease in the MB peak with respect to concentration (Fig. 3C) follows eqn (1) with a regression coefficient as −0.99611 and standard deviation of 0.06602, respectively.

$$\text{th-dsDNA} = -0.14637[\ln(1/\text{th-dsDNA concentration})] + 3.22364 \quad (1)$$

It may be noted that we have not observed any change in the MB peak height after hybridization with the target DNA < 0.000704 fmol, hence the detection limit of the th-ssDNA–ZnO/ITO electrode is 0.000704 fmol with the hybridization time of 60 s.

Conclusions

The sol–gel ZnO nano-porous film has been successfully deposited onto a glass substrate *via* dip-coating. The spectroscopic and electrochemical measurements show that the sol–gel derived nano-structured ZnO film is an excellent matrix for the immobilization of th-ssDNA onto the ZnO/ITO electrode surface for DNA hybridization detection. The relatively high sensitivity of the sol–gel derived ZnO matrix is due to the high surface area of nano-porous ZnO nanoparticles. The sol–gel nano-structured th-ssDNA–ZnO/ITO bioelectrode exhibits linearity in the range of 0.000524 fmol–0.524 nmol, with a detection limit of 0.000704 fmol and a hybridization time of 60 s. Efforts should be made to utilize this nucleic acid electrode for detection of gonorrhoea (STD) using clinical samples. This nucleic acid sensor has implications towards the clinical diagnosis of other sexually transmitted diseases.

Acknowledgements

We thank Dr Vikram Kumar, Director, NPL, New Delhi, India for facilities. Financial support received under the Department of Science and Technology (DST) projects (DST/TSG/ME/2008/18 and GAP- 070932), in-house project (OLP-070632D) and the DBT project (GAP-070832), are sincerely acknowledged. Thanks

are due to Dr Seema Sood and Rachna Prasad (AIIMS, New Delhi), and members of DSTCBE for interesting discussions.

References

1 A. Alam, M. Miah, M. Rahman, H. Sattar and A. Saleh, *Indian Journal of Medical Microbiol.*, 2002, **20**, 37–39.
2 J. Wang, *Nucleic Acid Research*, 2000, **28**, 3011–3016.
3 J. M. Nam, S. I. Stoeva and C. A. Mirkin, *J. Am. Chem. Soc.*, 2004, **126**, 5932–5933.
4 K. Arora, N. Prabhakar, S. Chand and B. D. Malhotra, *Anal. Chem.*, 2007, **79**, 6152–6158.
5 K. Arora, N. Prabhakar, S. Chand and B. D. Malhotra, *Biosens. & Bioelectron.*, 2007, **23**, 613–620.
6 L. Shen, Z. Chen, Y. Li, S. He, S. Xie, X. Xu, Z. Liang, X. Meng, Q. Li, Z. Zhu, M. Li, X. C. Le and Y. Shao, *Anal. Chem.*, 2008, **80**, 6323–6328.
7 J. Liu, S. Tian, P. E. Nielsen and W. Knoll, *Chem Commun.*, 2005, 2969–2971.
8 K. J. Odenthal and J. J. Gooding, *Analyst*, 2007, **132**, 603–610.
9 S. Shrestha, C. M. Y. Yeung, C. E. Mills, J. Lewington and S. C. Tsang, *Angew. Chem., Int. Ed.*, 2007, **119**, 1–6.
10 J. Wang, D. Xu and R. Polsky, *J. Am. Chem. Soc.*, 2002, **124**, 4208–4209.
11 G. Marrazza, I. Chianella and M. Mascini, *Biosens. & Bioelectron.*, 1999, **14**, 43–51.
12 N. Zhu, A. Zhang, Q. Wang, P. He and Y. Fang, *Anal. Chim Acta*, 2004, **510**, 163–168.
13 K. J. Feng, Y. H. Yang, Z. J. Wang, J. H. Jiang, G. L. Shen and R. Q. Yu, *Talanta*, 2006, **70**, 561–565.
14 Z. M. Liu, Y. L. Liu, G. L. Shen and R. Q. Yu, *Anal. Lett.*, 2008, **41**, 1083–1095.
15 X. Chen and S. Dong, *Biosens. & Bioelectron.*, 2003, **18**, 999–1004.
16 A. A. Ansari, A. Kaushik, P. R. Solanki and B. D. Malhotra, *Electrochem. Commun.*, 2008, **10**, 1246–1249.
17 A. A. Ansari, P. R. Solanki and B. D. Malhotra, *Appl. Phys. Lett.*, 2008, **92**, 263901–3.
18 E. Topoglidis, Y. Astuti, F. Duriaux, M. Gratzel and J. R. Durrant, *Langmuir*, 2003, **19**, 6894–6900.
19 A. Wei, X. W. Suna, J. X. Wang, Y. Lei, X. P. Cai, C. M. Li, Z. L. Dong and W. Huang, *Appl. Phys. Lett.*, 2006, **89**, 123902–3.
20 R. Khan, A. Kaushik, P. R. Solanki, A. A. Ansari, M. K. Pandey and B. D. Malhotra, *Anal. Chim. Acta*, 2008, **616**, 207–213.
21 J. J. Schneider, R. C. Hoffmann, J. Engstler, O. Soffke, W. Jaegermann, A. Issanin and A. Klyszcz, *Adv. Mater.*, 2008, **20**, 3383–3387.
22 L. Irimpan, V. P. N. Nampoori, P. Radhakrishnan, A. Deepthy and B. Krishnan, *J. Appl. Phys.*, 2007, **102**, 063524–6.
23 X. Chen, Y. Wang, J. Zhou, W. Yan, X. Li and J.-J. Zhu, *Anal. Chem.*, 2008, **80**, 2133–2140.
24 Q. Li, G. Luo, J. Feng, Q. Zhou, L. Zhang and Y. Zhu, *Electroanalysis*, 2001, **13**, 413–416.
25 J. C. Liao, M. Mastali, Y. Li, V. Gau, M. A. Suchard, J. Babbitt, J. Gornbein, E. M. Landaw, E. R. B. McCabe, B. M. Churchill and D. A. Haake, *J. Molecular Diagnostics*, 2007, **9**, 158–168.
26 K. Kerman, D. Ozkan, P. Kara, B. Meric, J. J. Gooding and M. Ozsoz, *Anal. Chim. Acta*, 2002, **462**, 39–47.
27 A. Erdem, K. Kerman, B. Meric, U. S. Akarca and M. Ozsoz, *Anal. Chim. Acta*, 2000, **422**, 139–149.
28 Y. Liu, M. Zhong, G. Shan, Y. Li, B. Huang and G. Yang, *J. Phys. Chem. B*, 2008, **112**, 6484–6489.

